

# Platelet-Derived Growth Factor Production by B16 Melanoma Cells Leads to Increased Pericyte Abundance in Tumors and an Associated Increase in Tumor Growth Rate

Masao Furuhashi,<sup>1</sup> Tobias Sjöblom,<sup>1</sup> Alexandra Abramsson,<sup>2</sup> Jens Ellingsen,<sup>1</sup> Patrick Micke,<sup>1</sup> Hong Li,<sup>3</sup> Erika Bergsten-Folestad,<sup>3</sup> Ulf Eriksson,<sup>3</sup> Rainer Heuchel,<sup>1</sup> Christer Betsholtz,<sup>2</sup> Carl-Henrik Heldin,<sup>1</sup> and Arne Östman<sup>1</sup>

<sup>1</sup>Ludwig Institute for Cancer Research, Uppsala Branch, Uppsala, Sweden; <sup>2</sup>Department of Medical Biochemistry, University of Göteborg, Göteborg, Sweden; and <sup>3</sup>Ludwig Institute for Cancer Research, Stockholm Branch, Stockholm, Sweden

## ABSTRACT

Platelet-derived growth factor (PDGF) receptor signaling participates in different processes in solid tumors, including autocrine stimulation of tumor cell growth, recruitment of tumor stroma fibroblasts, and stimulation of tumor angiogenesis. In the present study, the B16 mouse melanoma tumor model was used to investigate the functional consequences of paracrine PDGF stimulation of host-derived cells. Production of PDGF-BB or PDGF-DD by tumor cells was associated with an increased tumor growth rate. Characterization of tumors revealed an increase in pericyte abundance in tumors derived from B16 cells producing PDGF-BB or PDGF-DD. The increased tumor growth rate associated with PDGF-DD production was not seen in mice expressing an attenuated PDGF  $\beta$ -receptor and was thus dependent on host PDGF  $\beta$ -receptor signaling. The increased pericyte abundance was not associated with an increased tumor vessel density. However, tumor cell apoptosis, but not proliferation, was reduced in tumors displaying PDGF-induced increased pericyte coverage. Our findings thus demonstrate that paracrine PDGF production stimulates pericyte recruitment to tumor vessels and suggest that pericyte abundance influences tumor cell apoptosis and tumor growth.

## INTRODUCTION

Platelet-derived growth factors (PDGFs) are a family of dimeric disulfide-bonded growth factors exerting their biological effects through activation of two structurally related tyrosine kinase receptors, the PDGF  $\alpha$ - and  $\beta$ -receptors (1). In solid tumors, PDGF receptor signaling participates in various processes, including autocrine stimulation of tumor cell growth, recruitment of tumor stroma fibroblasts, and stimulation of tumor angiogenesis (reviewed in Ref. 2). The interest in exploiting PDGF signaling in tumors for therapeutic purposes has been intensified by the availability of clinically useful PDGF antagonists, such as STI571/Glivec (3–5).

For almost two decades, PDGF-AA, PDGF-AB, and PDGF-BB were the only known PDGF isoforms. However, two new PDGF isoforms, PDGF-CC and PDGF-DD, were identified recently (6–8). The novel PDGF isoforms are, in contrast to the classical PDGFs, synthesized and secreted as latent factors that are activated on proteolytic removal of a CUB domain that is localized in the NH<sub>2</sub>-terminal of the precursor protein.

Ligand binding to PDGF receptors entails receptor dimerization, kinase activation, and initiation of downstream signaling events. The

PDGF receptors are expressed on multiple cell types of mesenchymal origin, *e.g.*, fibroblasts, smooth muscle cells, pericytes, and glial cells (9).

The PDGF isoforms differ in their receptor specificity, *i.e.*, the A- and C-chains of PDGF bind only to PDGF  $\alpha$ -receptors, and the D-chain binds only to  $\beta$ -receptors, whereas the B-chain binds to both receptor types (6–8). PDGF-AB, PDGF-CC, and PDGF-DD activate both receptor types in cells that coexpress PDGF  $\alpha$ - and  $\beta$ -receptors, presumably reflecting ligand-induced receptor heterodimerization (7, 10).

Inhibition of tumor growth in experimental models of autocrine PDGF growth stimulation has been observed after blockage of PDGF receptor signaling, *e.g.*, in dermatofibrosarcoma protuberans and glioblastoma multiforme (11–15). Most recently, therapeutic effects have also been observed in dermatofibrosarcoma protuberans patients after treatment with PDGF receptor kinase inhibitors (16, 17). Paracrine PDGF stimulation also enhances tumor growth through recruitment of a vascularized stroma (18, 19). PDGF receptor signaling in tumor stromal cells was also recently shown to increase tumor interstitial fluid pressure and thereby hamper tumor uptake of anticancer drugs (20–22).

Finally, proangiogenic effects of PDGF have been described in various angiogenesis models (23–25). Studies on genetically altered mice deficient in PDGF  $\beta$ -receptor or PDGF B-chain production have also highlighted the importance of PDGF  $\beta$ -receptors on pericytes (26–28). PDGF  $\beta$ -receptor expression on tumor vessel pericytes has been described in both experimental tumors and human cancers (29, 30). Expression of PDGF  $\beta$ -receptors on tumor endothelial cells has also been described, *e.g.*, in capillaries of human glioblastomas and in experimental prostate bone metastases (31, 32). Direct evidence for tumor angiogenic effects of PDGFs was obtained recently with the demonstration of increased tumor angiogenesis after transfections of PDGF isoforms into NIH3T3 cells or U87MG glioma cells (33, 34). The antiangiogenic effects of STI571 in experimental bone metastases provide additional support for a role of PDGF receptor signaling in tumor angiogenesis (32).

In the present study, we have characterized the functional effects of PDGF stimulation of tumor pericytes in the B16 melanoma tumor model. We demonstrate that paracrine PDGF stimulation of pericytes in the B16 melanoma mouse tumor model leads to an increased pericyte abundance in tumor vessels and to an increase in tumor growth rate, which occurs in the absence of increase in vessel density.

## MATERIALS AND METHODS

**Cell Culture and Generation of Cell Lines Stably Expressing PDGF-BB or PDGF-DD.** B16F10 melanoma cells (American Type Culture Collection) were cultured in DMEM supplemented with 10% fetal bovine serum and antibiotics. Expression plasmids encoding full-length human PDGF-B and murine PDGF-D were generated by cloning of *PDGFB* and *PDGFD* cDNAs into the mammalian expression vector pcDNA3.1(+)-Zeo (Invitrogen). To

Received 5/25/03; revised 1/19/04; accepted 2/12/04.

Grant support: Swedish Cancer Foundation provided support for C. Betsholtz and A. Östman. IngaBritt and Arne Lundberg Foundation and Association for International Cancer Research, United Kingdom also supported C. Betsholtz and A. Abramsson.

The costs of publication of this article were defrayed in part by the payment of page charges. This article must therefore be hereby marked *advertisement* in accordance with 18 U.S.C. Section 1734 solely to indicate this fact.

Note: T. Sjöblom is currently at The Sidney Kimmel Cancer Center, Johns Hopkins University School of Medicine, Baltimore, Maryland.

Requests for reprints: Arne Östman, Ludwig Institute for Cancer Research, Uppsala Branch, Box 595, SE-751 24 Uppsala, Sweden. Phone: 46-18-16-04-14; Fax: 46-18-16-04-20; E-mail: arne.ostman@licr.uu.se, arne.ostman@cck.ki.se.

obtain stable expression, 60–80% confluent B16F10 cells were transfected with pcDNA3.1(+)-Zeo, pcDNA3.1(+)-Zeo-hPDGF-B, or pcDNA3.1(+)-Zeo-mPDGF-D using LipofectAMINE reagent (Invitrogen). After 3 weeks of selection in Zeocin (Invitrogen), resistant mass cultures were isolated and propagated as cell lines (B16/ctr, B16/PDGF-B, and B16/PDGF-D) under continuous Zeocin selection.

**Analysis of PDGF-DD and PDGF-BB Expression.** Reverse transcription-PCR for detection of PDGF-D mRNA in PDGF-D-transfected cells was performed according to standard procedures. For analyses of the expression of PDGF-DD, conditioned media were collected from subconfluent cultures of B16/ctr and B16/PDGF-D cultured for 12 h in serum-free medium, and total protein was recovered by precipitation in 20% trichloroacetic acid for 1 h on ice. Precipitated proteins were solubilized in SDS sample buffer and separated by SDS-PAGE. After electrophoretic transfer to nitrocellulose membrane (Hybond-C; Amersham), PDGF-DD was detected by immunoblotting with 2  $\mu$ g/ml of an affinity-purified PDGF-DD antibody (6).

For PDGF-BB detection, subconfluent cultures of B16/ctr and B16/PDGF-B cells were metabolically labeled for 8 h in serum-free MCDB104 medium supplemented with 100  $\mu$ Ci of [ $^{35}$ S]cysteine (Amersham). Conditioned media were collected, and cells were lysed in 0.5 M NaCl, 0.01 M Tris (pH 7.8), 0.5% Triton X-100, 1% aprotinin, and 1 mM phenylmethylsulfonyl fluoride. Subsequently, PDGF-BB was immunoprecipitated from supernatants and cell lysates using rabbit anti-PDGF-BB antiserum (35), followed by incubation with protein A-Sepharose (Amersham). After four washes in 0.5 M NaCl, 1% Triton X-100, 0.01 M Tris (pH 7.5), 5 mg/ml BSA, and 0.1% SDS, bound proteins were eluted by boiling in nonreducing or reducing SDS sample buffer and separated by SDS-PAGE.

**Analyses of PDGF  $\beta$ -Receptor Stimulatory Activity in Conditioned Media of B16/ctr, B16/PDGF-B, and B16/PDGF-D Cells.** Conditioned media were collected from subconfluent cultures of B16/ctr, B16/PDGF-B, and B16/PDGF-D cells, cultured for 72 h in serum-free medium, and concentrated five times by Centrplus (Millipore). PDGF  $\beta$ -receptor phosphorylation induced by the conditioned media or by recombinant PDGF-BB in PAE/PDGF $\beta$  cells was analyzed as described previously (20).

**Characterization of *in Vitro* Growth and Analyses of PDGF  $\beta$ -Receptor Expression on B16 Cells *in Vitro*.** B16/ctr, B16/PDGF-B, or B16/PDGF-D cells ( $5 \times 10^4$  cells/well) were plated in 24-well plates (Sarstedt) in DMEM in the absence or presence of 10% FCS. Media were changed three times per week. Every 3 days after seeding, triplicate wells of cells were trypsinized and counted using a Coulter particle counter. PDGF  $\beta$ -receptor expression and phosphorylation were analyzed as described previously (21).

**Tumor Formation Assay.** Animal experiments were approved by the local ethical committee and performed according to the United Kingdom Coordinating Committee on Cancer Research guidelines (36). All manipulations were performed in isoflurane gas anesthesia. Twelve 13-week-old C57Bl6/J mice received s.c. inoculation in the dorsal skinfold with  $1 \times 10^6$  B16/ctr ( $n = 10$ ), B16/PDGF-B ( $n = 9$ ), or B16/PDGF-D ( $n = 10$ ) cells dissolved in 100  $\mu$ l of PBS. C57Bl6/J mice expressing a PDGF  $\beta$ -receptor deficient in phosphatidylinositol 3'-kinase recruitment (Y739F/Y750F mice; Ref. 37) received injection with  $1 \times 10^6$  B16/ctr ( $n = 10$ ) or B16/PDGF-D ( $n = 10$ ) cells dissolved in 100  $\mu$ l of PBS. Tumor length and width were measured every 3 days using calipers, and tumor volume was calculated as  $\pi/6 \times \text{length} \times \text{width}^2$ . At days 13 or 17 after inoculation, animals were sacrificed by i.p. injection of 90 mg/kg $^{-1}$  pentobarbitone, followed by perfusion through the left cardiac ventricle with 10 ml of PBS (pH 7.4), followed by perfusion fixation with 20 ml of 4% paraformaldehyde in PBS. Tumors were subsequently removed surgically, weighed, and fixed in paraformaldehyde overnight. After embedding tumors in paraffin, sections were cut at 4- $\mu$ m thickness onto Superfrost Plus slides (Histolab). For confocal microscopy, tumors were fixed in 4% paraformaldehyde, cryoprotected in 30% sucrose, frozen, and cut into sections 14- $\mu$ m thick.

**Histochemistry, Immunohistochemistry, and Stereological Analyses of Tumor Vessels.** Overview histology and connective tissue content were visualized by Azan trichrome staining (Bio-Optica) of deparaffinized tissue sections. For immunohistochemistry, sections were deparaffinized and pretreated by boiling in 10 mM citrate buffer (pH 6.0) or in target retrieval solution (high pH; DAKO) for  $2 \times 7$  min at 750 W in a microwave oven. Tissue peroxidase activity was quenched by incubation in 3% H<sub>2</sub>O<sub>2</sub> in PBS for 10 min, followed by blocking in 20% serum of the secondary antibody species.

Capillary blood vessel immunohistochemistry was performed with goat anti-mouse CD31/platelet/endothelial cell adhesion molecule 1 (PECAM-1) antibody (1  $\mu$ g/ml sc-1506; Santa Cruz Biotechnology). PDGF  $\beta$ -receptor immunohistochemistry was performed with 958 rabbit anti-PDGF  $\beta$ -receptor antiserum (1  $\mu$ g/ml sc-432; Santa Cruz Biotechnology) using a procedure that has been validated by demonstrating the absence of staining in PDGF  $\beta$ -receptor knockout mice embryos.<sup>4</sup> Omission of primary antibody was used as a negative control.  $\alpha$ -Smooth muscle actin (ASMA) was detected with horseradish peroxidase-conjugated monoclonal 1A4 antibody (EPOS ASMA; Dako). For double staining of pericytes and endothelial cells, unconjugated 1A4 ASMA monoclonal antibodies (1  $\mu$ g/ml; Dako) and goat antimouse CD31/PECAM-1 antibodies (1  $\mu$ g/ml sc-1506; Santa Cruz Biotechnology) were used consecutively. ASMA antibodies were detected with biotinylated rabbit antimouse antibodies visualized by Vectastain ABC-AP kit (Vector Laboratories). CD31 antibodies were detected with biotinylated rabbit anti-goat antibodies visualized by Vectastain ABC kit (Vector Laboratories). Apoptotic cell and proliferative cell immunohistochemistry were performed with cleaved caspase-3 antibody (Cell Signaling Technology) and Ki67 antibody (MIB5; Immunotech). The fraction of cleaved caspase-3-positive cells or Ki67-positive cells was determined after analyzing 1000 cells on all tumors from each group. Positive reactions were developed using 3,3'-diaminobenzidine (Vector Laboratories) as a peroxidase substrate and nitroblue tetrazolium/5-bromo-4-chloro-3-indolyl phosphate (Roche) as an alkaline phosphatase substrate. Sections were counterstained in Mayer's hematoxylin, dehydrated, and coverslipped in Mountex resin (Histolab). Tumor cell density, determined on all tumors from each group, was quantified by counting the numbers of cells in three or four fields of vision (0.09 mm<sup>2</sup>) of viable tissue. Stereological quantification of capillary tumor blood vessels was performed after CD31 staining, as described previously (11, 38, 39). The number of pericyte nuclei associated with tumor vessels was counted after single staining with ASMA or PDGF  $\beta$ -receptor in 10 randomly selected fields of vision of 0.09 mm<sup>2</sup>. Analyses of pericyte numbers after double staining were performed by counting pericytes in whole tumor sections. All immunohistochemical analyses were performed on five tumors from each group (except for B16/PDGF-D tumors from mutant mice, for which four tumors were analyzed), after exclusion of the largest and smallest tumors from each group.

Confocal analyses was performed with rat anti-CD31/PECAM-1 (Phar-Mingen), rabbit anti-NG2 (Chemicon), FITC-conjugated mouse ASMA antibodies (Sigma), and secondary antibodies conjugated with the appropriate fluorochrome (Alexa 488, 568, or 633; Molecular Probes) for labeling of endothelial cells and vascular smooth muscle cells/pericytes. Mounted sections were analyzed by confocal laser scanning microscopy using a Leica TCS NT. Digital images were processed using Adobe Photoshop 6.0.

**Statistical Analysis.** Statistical analysis was performed using ANOVA.  $P < 0.05$  was considered as statistically significant.

## RESULTS

**PDGF  $\beta$ -Receptor Expression in B16 Tumors Is Restricted to Pericytes.** To validate the B16 tumor as a model to study potential effects of paracrine PDGF stimulation, tissue sections from B16 tumors were subjected to immunohistochemical analyses using antibodies recognizing PDGF  $\beta$ -receptor, ASMA, and CD31 (Fig. 1, A–C). As shown in Fig. 1, A and B, neovessels in B16 melanoma were associated with ASMA-positive mural cells and showed prominent perivascular PDGF  $\beta$ -receptor staining. In contrast to the endothelial cell labeling by CD-31/PECAM-1 immunohistochemistry (Fig. 1C), the vascular PDGF  $\beta$ -receptor staining was discontinuous and peripheral with endothelial cell bodies at the luminal side. The only PDGF  $\beta$ -receptor-positive cells seen in B16 tumors were closely associated with vessels, most likely representing pericytes and possibly perivascular fibroblasts. The presence of pericytes, giving rise to a partial pericyte coverage of tumor vessels, in B16 tumors was shown by confocal analyses of tumor sections stained with antibodies against CD31 and ASMA (Fig. 1D).

<sup>4</sup> T. Sjöblom, unpublished observations.

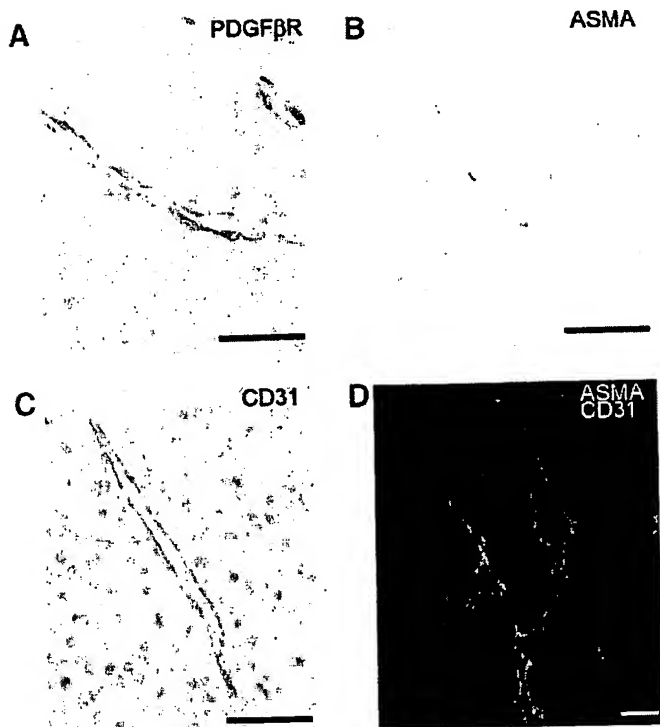


Fig. 1. Perivascular expression of the platelet-derived growth factor (PDGF)  $\beta$ -receptor in B16 melanoma tumors. A–C, paraffin-embedded tissue sections from control-transfected B16 melanoma tumors were stained using antibodies to the pericyte marker PDGF  $\beta$ -receptor (A),  $\alpha$ -smooth muscle actin (ASMA; B), and endothelial cell marker CD31 (C). A characteristic abluminal and incomplete staining pattern is present in ASMA and PDGF  $\beta$ -receptor immunostaining, in contrast to the luminal CD31 positivity that completely surrounds the capillary cross section. No other PDGF  $\beta$ -receptor-positive cell type was detected in the tumors. D, confocal image of vessel segment from control-transfected B16 melanoma tumors double stained for CD31 (red) and ASMA (green). Scale bars, 50  $\mu$ m.

**Establishment of B16 Cell Lines Producing PDGF-BB or PDGF-DD.** To study the effects of tumor-derived PDGF  $\beta$ -receptor agonists on the recruitment of pericytes to the tumor vessels, B16 melanoma cells were transfected with control plasmid or plasmids encoding full-length PDGF-B or PDGF-D. After selection, mass cultures derived from 20–30 clones were analyzed with regard to expression of PDGF-BB and PDGF-DD.

Expression of *PDGFD* mRNA in transfected cells was analyzed by reverse transcription-PCR. As shown in Fig. 2A, a PCR product of the expected size of 350 bp was detected in the positive control reaction and when cDNA from *PDGFD*-transfected cells was used. PDGF-DD expression was also confirmed by immunoblotting (Fig. 2B). Under reducing conditions, PDGF-D antibodies detected a component of  $M_r$  55,000 in conditioned medium from *PDGFD*-transfected cells, which was absent in medium from control-transfected cells. Based on comparisons with similar analyses of recombinant full-length and cleaved PDGF-D, the  $M_r$  55,000 protein is most likely the full-length uncleaved form of PDGF-DD (6).

PDGF-BB expression was analyzed by immunoprecipitation from metabolically labeled cell lysates and conditioned media, followed by SDS-PAGE. PDGF-BB antibodies precipitated components of  $M_r$  50,000,  $M_r$  40,000,  $M_r$  35,000, and  $M_r$  24,000 from the cell lysate and components of  $M_r$  30,000 and  $M_r$  24,000 from the conditioned medium of *PDGFB*-transfected cells, but not from control-transfected cells, as analyzed under nonreducing conditions (Fig. 2C, left panel). Components of similar size were also detected in precipitates from previously established *PDGFB*-transfected NIH3T3 cells, which were included as a positive control (data not shown). When analyzed under reducing conditions, the components specific for the *PDGFB*-trans-

fected cells were converted to species of  $M_r$  20,000,  $M_r$  16,000, and  $M_r$  12,000 in the lysate and  $M_r$  16,000 in the conditioned medium (Fig. 2C, right panel), consistent with formation of processed PDGF-BB dimers in transfected B16 cells.

To further characterize the transfected cells, conditioned media were collected and analyzed with regard to content of PDGF  $\beta$ -receptor stimulatory activity. As shown in Fig. 2D, conditioned media from B16/PDGF-B cells, in contrast to B16/ctr and B16/PDGF-D cells, induced strong PDGF  $\beta$ -receptor phosphorylation.

We thus conclude, from the results in Fig. 2, that the B16/PDGF-B cells produce functional PDGF-BB and that the PDGF-DD produced by B16/PDGF-D cells is secreted as a latent product.

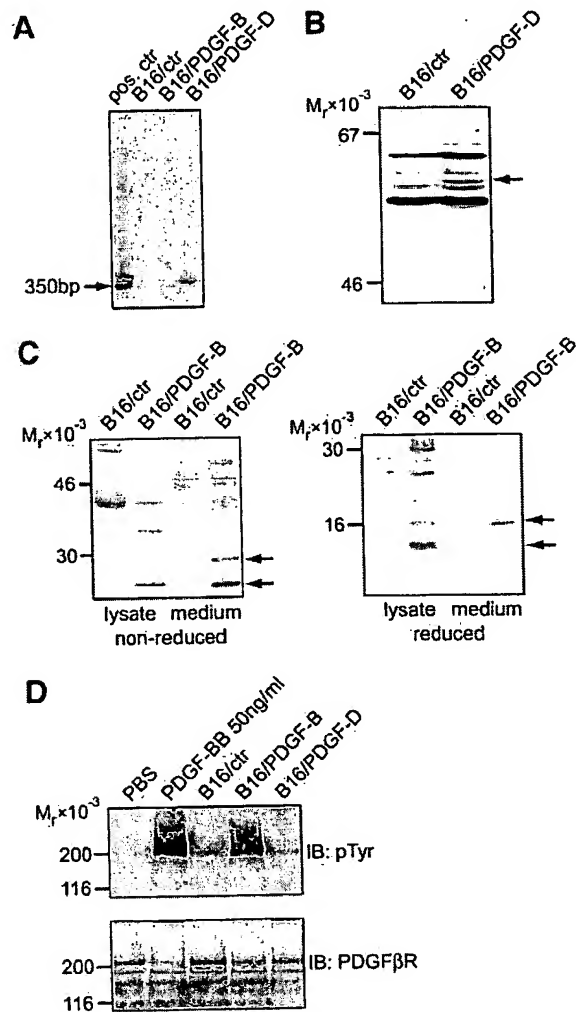


Fig. 2. Platelet-derived growth factor (PDGF)-BB and PDGF-DD expression in transfected B16 melanoma cells. A, cDNA was generated from B16/ctr, B16/PDGF-B, and B16/PDGF-D cell polyadenylated RNA, respectively, followed by PCR amplification with *PDGFD*-specific primers and agarose gel electrophoresis. Amplification products from *PDGFD* control DNA (Lane 1), B16/ctr cells (Lane 2), B16/PDGF-B cells (Lane 3), and B16/PDGF-D cells (Lane 4) were separated by agarose gel electrophoresis. B, total protein in conditioned media from mock-transfected or *PDGFD*-transfected B16 cells were recovered by trichloroacetic acid precipitation. After SDS-PAGE under reducing conditions in a 10% gel and electrophoretic transfer, the blotting membrane was probed with rabbit antiserum to PDGF-DD. Arrow indicates migratory position of reduced precursor form of PDGF-DD. C, control-transfected or *PDGFB*-transfected B16 melanoma cells were metabolically labeled with [ $^{35}$ S]cysteine for 8 h. Lysates and conditioned media were immunoprecipitated with PDGF-BB antiserum and analyzed under nonreducing (left panel) or reducing (right panel) conditions by SDS-PAGE in 10% and 15% gels, respectively. Positions of molecular weight markers are indicated to the left. D, subconfluent cultures of porcine aortic endothelial cells transfected with PDGF  $\beta$ -receptor (*PAE/PDGFR $\beta$* ) were stimulated with conditioned media of B16/ctr, B16/PDGF-B, or B16/PDGF-D cells. PDGF  $\beta$ -receptor was immunoprecipitated from cell lysates, and receptor tyrosine phosphorylation was determined by phosphotyrosine immunoblotting.

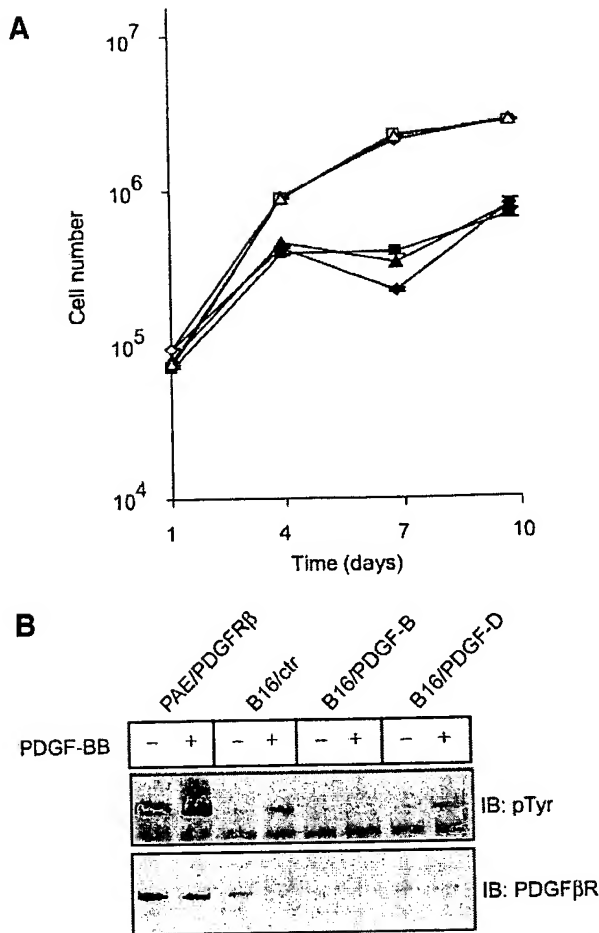


Fig. 3. Expression of platelet-derived growth factor (PDGF)-BB or PDGF-DD does not affect the *in vitro* growth rate of B16 melanoma cells. A, B16/ctr (squares), B16/PDGF-B (triangles), or PDGF-D (circles) cells were seeded in 24-well plates and cultured in the absence (closed symbols) or presence (open symbols) of 10% FCS. At the indicated times, cells were trypsinized, and cell number was determined with a Coulter counter. Results are presented as mean  $\pm$  SD of quadruplicate measurements and are representative of three independent experiments. B, PDGF  $\beta$ -receptor expression in B16/ctr, B16/PDGF-B, and B16/PDGF-D cells was analyzed by PDGF  $\beta$ -receptor (PDGFR $\beta$ ) and phospho-tyrosine (pTyr) immunoblotting of wheat germ agglutinin fractions. Porcine aortic endothelial cells transfected with PDGF  $\beta$ -receptor (PAE/PDGF $\beta$ R) were included as a positive control.

**Paracrine PDGF-BB and PDGF-DD Stimulation of Pericytes Enhances Tumor Growth.** Before analyses of the effects of PDGF transfection into B16 cells *in vivo*, the growth *in vitro* of PDGFB- and PDGFD-transfected cells was analyzed. As shown in Fig. 3A, no difference in the *in vitro* growth rate among the three cell lines was detected in either the absence or presence of 10% FCS. Cultured B16 cells were also analyzed with regard to PDGF  $\beta$ -receptor expression. A low level of expression of PDGF  $\beta$ -receptors was detected on control cells and in transfected cells, which could be activated by the addition of a high concentration of exogenous ligand (Fig. 3B). The PDGF-transfected cells appeared to show an even lower expression than the control cells, possibly reflecting ligand-induced down-regulation of receptors. Binding studies with radioactively labeled PDGF indicated that receptor expression in control cells was  $<5\%$  of the expression seen in PDGF-responsive human fibroblasts (data not shown).

The effects of paracrine PDGF-BB and PDGF-DD expression on B16 melanoma tumor growth were analyzed in two independent experiments by monitoring tumor growth rate in C57B16/J mice after s.c. injection of tumor cells. In the first experiment, tumors were allowed to grow 13 days after tumor cell injection (13-day study), and

in the second experiment, animals were sacrificed 17 days (17-day study) after tumor cell injection (Fig. 4, A and B). In both experiments, the mean volumes of tumors derived from B16/PDGF-B cells were significantly increased as compared with tumors from control-transfected cells at the time of sacrifice (Fig. 4, A and B). Also, B16/PDGF-D tumors grew faster than control tumors and were significantly bigger than control tumors at day 17 (Fig. 4, A and B).

The very low levels of PDGF  $\beta$ -receptor expression on B16 melanoma cells and the lack of growth-stimulatory effects *in vitro* of PDGF transfections indicated that the significantly increased growth rate *in vivo* reflected a paracrine effect of the tumor-derived PDGF on host cells. To test this, B16/PDGF-D tumor formation was compared in wild-type mice and in mice in which wild-type  $\beta$ -receptor had been replaced by an attenuated PDGF  $\beta$ -receptor deficient in activation of phosphatidylinositol 3'-kinase (Y739F/Y750F mice). The PDGF-DD-producing cells were selected for this experiment because paracrine effects of PDGF-BB were predicted to be rescued by wild-type PDGF  $\alpha$ -receptors. As shown in Fig. 4C, expression of the attenuated PDGF  $\beta$ -receptor significantly decreased the growth rate of the B16/PDGF-D tumors, without reducing the growth of tumors derived from control cells.

These experiments thus demonstrate that paracrine PDGF  $\beta$ -receptor stimulation of perivascular host cells is associated with increased tumor growth rate.

**Paracrine PDGF-BB and PDGF-DD Effect on Tumor Growth Is Associated with Increased Pericyte Abundance in the Tumor Vasculature.** The results described above prompted a more detailed characterization of the tumor vessels. Because we were able to demonstrate significant PDGF  $\beta$ -receptor labeling only on perivascular cells of the tumor, we focused our interest on tumor vessel pericytes and the possibility that these cells are the primary targets of the tumor-derived PDGFs. Previous studies have shown that PDGF-BB regulates pericyte recruitment during embryonic development (27), and we therefore first characterized the pericyte abundance and association with the tumor vessels in the B16 control and transfected tumors.

Thick sections from B16/ctr, B16/PDGF-B, and B16/PDGF-D tumors were double stained with CD31 antibodies (as endothelial cell markers) and either NG2 or ASMA antibodies (as markers for pericytes) and analyzed by confocal laser scanning microscopy. NG2 and ASMA are both reported to stain tumor pericytes (30, 40–42), but some tumors have larger proportions of pericytes expressing NG2 than ASMA, suggesting that the expression of these two markers does not always overlap and that distinct populations or states of pericyte differentiation may coexist in the same tumor.<sup>5</sup> In addition, ASMA, but not NG2, stains tumor stroma fibroblasts (Fig. 5D, arrowheads). As shown in Fig. 5, clear differences were observed between the different tumors with regard to pericyte abundance using both ASMA and NG2 as pericyte markers. B16/ctr cells gave rise to tumors in which the vessels were poorly covered by pericytes (Fig. 5, left panels). In contrast, both B16/PDGF-B and B16/PDGF-D tumors were characterized by a vasculature with much higher density of associated pericytes (Fig. 5, middle and right panels). The pericytes in B16/PDGF-B and B16/PDGF-D tumors showed a different association with the abluminal endothelial surface compared with the control tumors. In the controls, the pericytes were tightly associated, whereas in the PDGF-expressing tumors, most of the pericytes appeared partially detached from the endothelial surface. Occasionally, completely detached cells were seen, which were judged to be pericytes rather

<sup>5</sup> A. Abramsson and C. Betsholtz, unpublished observations.

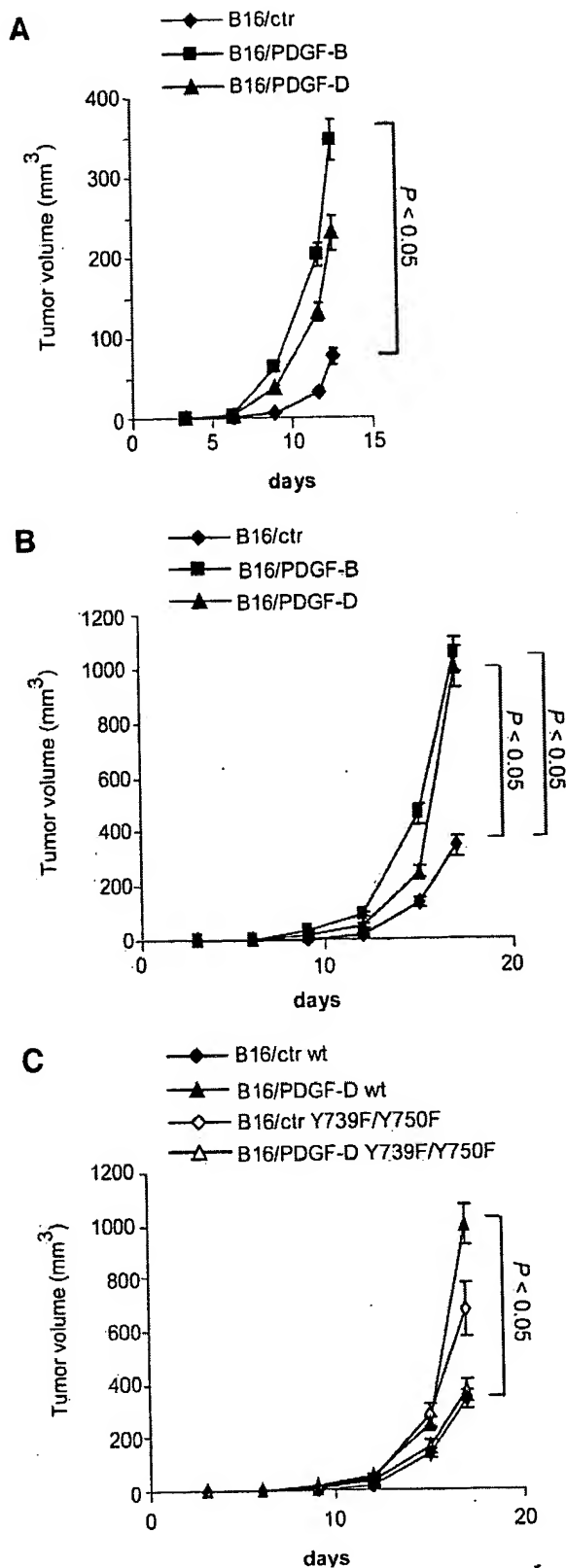


Fig. 4. Expression of platelet-derived growth factor (PDGF)-BB or PDGF-DD increases the growth rate of B16 melanoma *in vivo*. A and B, control-transfected B16 cells ( $\blacklozenge$ ) or cells transfected with PDGF-B ( $\blacksquare$ ) or PDGF-D ( $\blacktriangle$ ) were inoculated in the dorsal skinfold of C57B16/J mice. Tumor volume was measured every 3 days, and animals were sacrificed 13 (A) or 17 days (B) after tumor cell injection. C, control-transfected B16 cells (diamonds) or B16/PDGF-D cells (triangles) were inoculated in the dorsal skinfold of wild-type C57B16/J mice (wt; closed symbols) or mice expressing an attenuated PDGF  $\beta$ -receptor (Y739F/Y750F; open symbols). Results are presented as mean  $\pm$  SE. Analysis of statistical significance was performed by ANOVA.

than fibroblasts because of their morphology and positive staining for NG2 (Fig. 5, E, F, H and I, arrows).

The abundance of perivascular PDGF  $\beta$ -receptor-positive cells in the B16 control and B16/PDGF-B and B16/PDGF-D tumors was also quantified. These analyses were performed on paraffin sectioned material after PDGF  $\beta$ -receptor or ASMA staining (see Fig. 1, A and B, for examples). The number of pericyte nuclei associated with tumor vessels was determined. This quantification revealed a significantly higher number of PDGF  $\beta$ -receptor positive pericytes in B16/PDGF-B tumors at days 13 and 17 and in B16/PDGF-D tumors at day 17 as compared with B16/ctr tumors (Fig. 6A and B, right panels). Similar results were obtained when ASMA staining was used for pericyte detection (Fig. 6, A and B, right panels). Also, the pericyte abundance in B16/PDGF-D tumors in Y739F/Y750F mice expressing the attenuated PDGF  $\beta$ -receptor was significantly lower at day 17 as compared with tumors from the same cells in wild-type mice (Fig. 6B).

The tumors were also subjected to stereological analysis of the tumor vasculature. No increases in vessel length density were observed in the PDGF-producing tumors (Fig. 7). A reduction in volumetric and surface density was observed in the PDGF-B-producing tumors in the 13- and 17-day studies, respectively (Fig. 7, A and B). Mean section areas, diameters, or mean boundary lengths of vessels did not differ between the groups (data not shown).

To substantiate the indications that PDGF production by tumor cells was associated with increased pericyte coverage of tumor vessels occurring in the absence of increased vessel density, double staining with CD31 and ASMA antibodies was performed on sections of B16/ctr and B16/PDGF-B tumors from the 17-day study. Pericytes were counted, and stereological analyses were performed. In agreement with the findings of Fig. 7B, the analyses provided no evidence of increased vessel density in the PDGF-B-producing tumors (data not shown). Also in agreement with previous results, a significantly higher number of ASMA-positive cells, associated with CD31-positive cells, was observed in the B16/PDGF-B tumors at day 17 (Fig. 7C). An increased number of ASMA-positive cells, juxtaposed to vessels, was also seen at day 13 (data not shown). When the values from the quantification of endothelial cell-associated ASMA-positive cells were combined with the values from stereological quantification of vessel surface density, a significant increase in pericyte coverage of vessels was observed in B16/PDGF-B tumors at both day 13 and day 17 (data not shown).

In summary, the characterization of the tumor vasculature thus revealed that PDGF-BB and PDGF-DD production by tumor cells resulted in a PDGF  $\beta$ -receptor-dependent increase in tumor vessel pericyte abundance, which occurred in the absence of increase in tumor vessel density.

**Paracrine Stimulation of Tumor Pericytes Is Associated with a Decrease in Tumor Cell Apoptosis.** To investigate the consequences of the increased pericyte abundance on tumor cell apoptosis and proliferation, sections from B16/ctr, B16/PDGF-B, and B16/PDGF-D tumors from the 18-day study were stained with antibodies recognizing the apoptosis marker cleaved caspase-3 and the proliferation marker Ki67. These analyses revealed a significant reduction in tumor cell apoptosis but no changes in tumor cell proliferation in B16/PDGF-B and B16/PDGF-D tumors (Fig. 8, A and B). Finally, analysis of cell density revealed no differences among the three tumor groups (Fig. 8C). These data thus indicate that the increase in tumor size, which is associated with the increased pericyte coverage, occurs through reduction in tumor cell apoptosis.

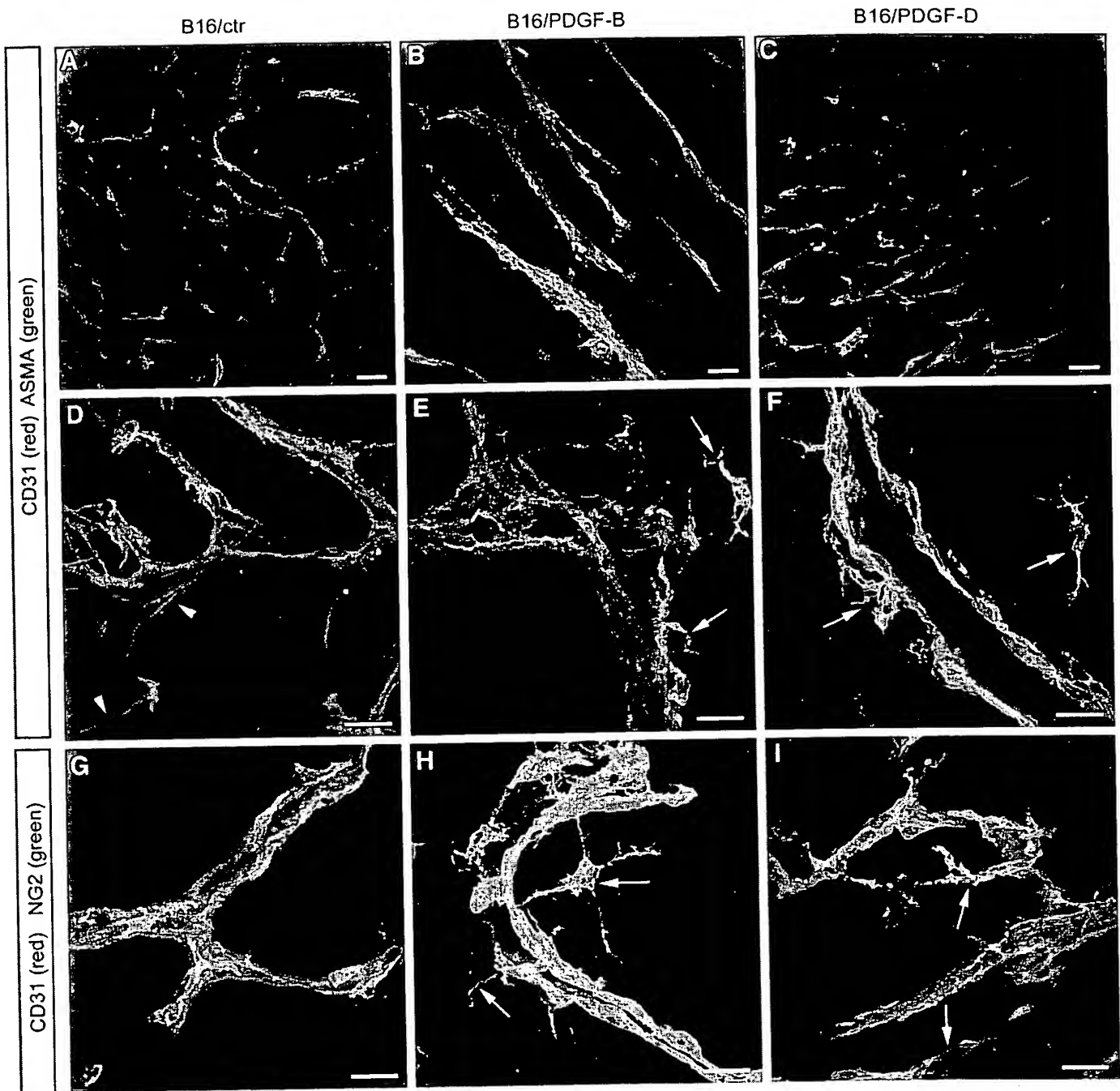


Fig. 5. Platelet-derived growth factor (PDGF) production by B16 cells changes pericyte recruitment in tumor vessels. Confocal analysis of sections double stained for endothelial cells (CD31, red) and pericytes ( $\alpha$ -smooth muscle actin or NG2, green) in the vasculature of tumors grown from control-transfected B16 cells (*B16/ctr*) or cells transfected with *PDGFB* (*B16/PDGF-B*) or *PDGFD* (*B16/PDGF-D*). Representative fields at overview (A–C) and high magnification (D–I) illustrate the increased density of pericytes/vascular smooth muscle cells surrounding the vessels of PDGF-BB- and PDGF-DD-expressing tumors. Vascular smooth muscle cells in PDGF-BB- and PDGF-DD-expressing tumors cell are spreading or detached (E, F, H, and I, arrows) as compared with the control tumor (D and G). Note that  $\alpha$ -smooth muscle actin also stains fibroblast-like cells located within the tumor (D, arrowheads). Scale bars: A–C, 50  $\mu$ m; D–I, 20  $\mu$ m.

## DISCUSSION

In summary, our study demonstrates that PDGF-BB or PDGF-DD production by tumor cells leads to an increase in tumor vessel pericyte abundance and enhances tumor growth rate in the absence of changes in vessel density. The effects of PDGF-DD, which only binds PDGF  $\beta$ -receptor, were abolished in mice expressing an attenuated  $\beta$ -receptor, thus demonstrating that the effects of paracrine PDGF stimulation in this model occur through effects on host-derived PDGF  $\beta$ -receptor-positive cells.

PDGF-DD secreted from transfected B16 cells occurred as a species of  $M_r$  55,000 under reducing conditions. According to previous analysis of full-length and processed PDGF-DD lacking the CUB domain, the  $M_r$  55,000 form corresponds to the uncleaved form (6). The notion that PDGF-DD secreted by B16 cells occurs as a latent protein was also supported by the absence of PDGF receptor stimulating activity in the conditioned medium of PDGF-DD-transfected cells. However, the phenotypic consequences of PDGF-DD expression clearly indicate biological activity of the protein in the tumor

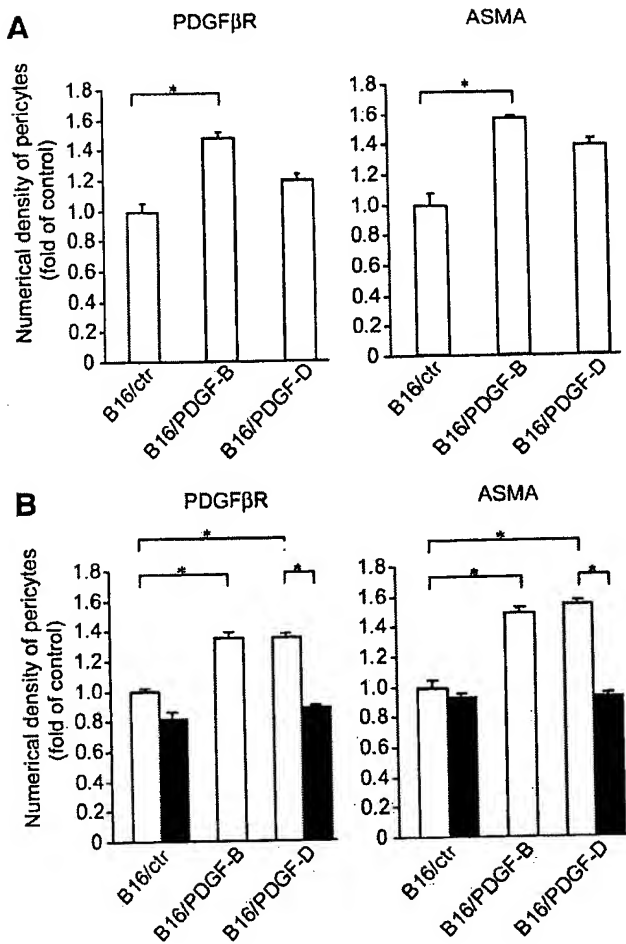


Fig. 6. Platelet-derived growth factor (PDGF) production by B16 cells increases the pericyte abundance in tumors in a PDGF  $\beta$ -receptor-dependent manner. Pericyte quantification was performed in tumors from the 13- (A) and 17-day (B) studies after PDGF  $\beta$ -receptor (left panels) or  $\alpha$ -smooth muscle actin (right panels) stainings. Pericyte nuclei around tumor vessels in wild-type mice ( $\square$ ) or Y739F/Y750F mice expressing an attenuated PDGF  $\beta$ -receptor ( $\blacksquare$ ) were counted in 10 randomly selected vision fields of 0.09 mm<sup>2</sup>. Results are presented as mean  $\pm$  SE. Analysis of statistical significance was performed by ANOVA; \*,  $P < 0.05$ .

model. A possible explanation for this is that latent PDGF-DD in the tumors is cleaved by proteases present in the tumor environment. An alternative possibility could be that PDGF-DD, in its uncleaved form, exerts some biological effects through as yet unidentified receptors. However, because production of PDGF-DD in the mice expressing an attenuated PDGF  $\beta$ -receptor failed to increase pericyte abundance or induce an increased tumor growth rate, the latter possibility remains less likely.

The effects of paracrine PDGF action have been investigated previously in other models. Expression of PDGF in WM9 melanoma cells or HaCaT cells leads to a stromal response (18, 19). Also, inhibition of PDGF-AA production in a desmoplastic breast cancer cell line reduced tumor fibrosis (43). Our investigations of the histology of the different B16 tumors did not reveal major changes in stromal content of tumors derived from control cells or from PDGF-producing cells. This might reflect intrinsic differences between the models studied, e.g., with regard to the production of factors cooperating with PDGF in recruitment of a fibroblast-rich stroma.

PDGF  $\beta$ -receptor activation has long been considered a candidate angiogenic stimulus in tumors based on the effects of PDGF in angiogenesis assays, e.g., rings of rat aorta, chick chorioallantoic membranes, and mouse corneal pocket assays (24, 25, 44). Several

studies support the notion that PDGF receptor signaling in pericytes or endothelial cells also contributes to tumor angiogenesis (32–34). A recent study demonstrated that PDGF-BB expressed by tumor endothelial cells directly controls pericyte recruitment and that endothelial retention of PDGF-BB is required to keep the pericytes tightly vessel-associated (45). However, the consequences for vessel function and tumor growth of the different pericyte densities were not addressed. It is noteworthy that the PDGF-induced increase in pericyte abundance occurs in the absence of increased vessel density. In contrast, the PDGF-BB-producing tumors were characterized by a significantly decreased volumetric and surface vessel density at the late and early time point, respectively. This finding was not entirely unexpected because it has previously been demonstrated that a reduced tumor

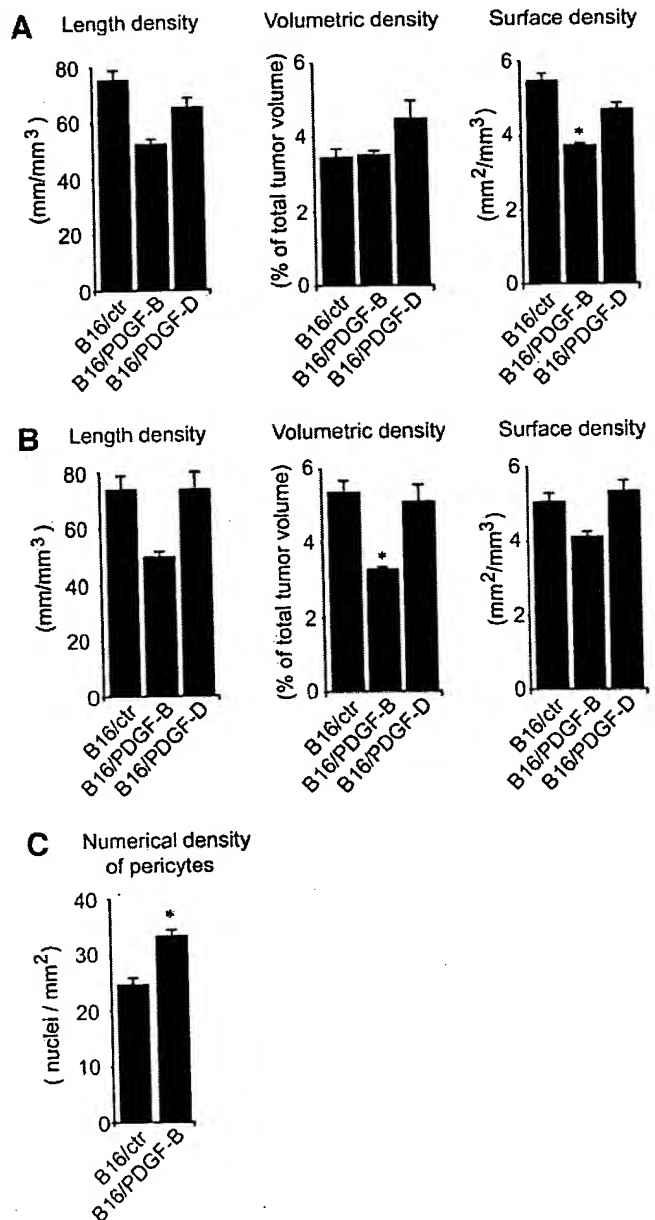


Fig. 7. Platelet-derived growth factor (PDGF)-BB or PDGF-DD production is not associated with increased vessel density. A and B, tumor blood vessel densities in tumors from the 13- and 17-day studies were characterized by stereological analysis after CD31 staining. C, sections from B16/ctr and B16/PDGF-B tumors from the 17-day study were also subjected to double staining with CD31 and  $\alpha$ -smooth muscle actin antibodies, and the density of  $\alpha$ -smooth muscle actin-positive cells associated with CD31-positive cells was quantified. All results are presented as mean  $\pm$  SE. Analysis of statistical significance was performed by ANOVA; \*,  $P < 0.05$ .

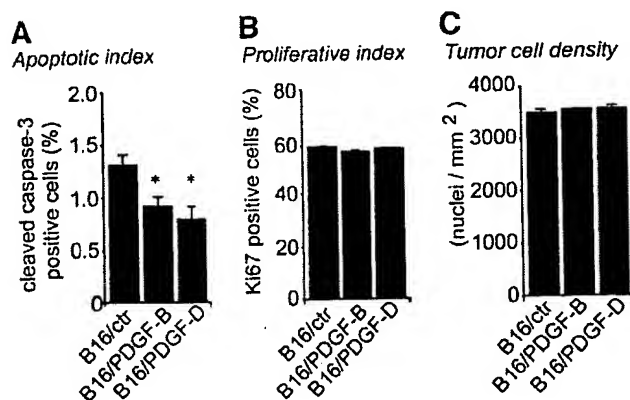


Fig. 8. Expression of platelet-derived growth factor BB or platelet-derived growth factor DD decreases tumor cell apoptosis, but not proliferation, in B16 tumors. A and B, apoptotic (A) and proliferative (B) index was determined by immunohistochemical staining with antibodies against cleaved caspase-3 and Ki67, respectively. C, tumor cell density was calculated by counting the numbers of cells in three or four fields of vision of 0.09 mm<sup>2</sup> of viable tissue. Results are presented as mean  $\pm$  SE. Analysis of statistical significance was performed by ANOVA; \*,  $P < 0.05$ .

vessel pericyte density is associated with increased vessel diameter and volumetric density (45).

With regard to the effects of PDGF production during different phases of tumor growth, it can be noted that the effects of PDGF production were stronger at the later time point in this experimental system; e.g., the PDGF-DD-producing tumors showed significantly increased tumor growth and pericyte abundance only at the later time point (Figs. 4 and 6). The significance of these differences remains unclear but could possibly reflect a pericyte-mediated protection from regression of immature vessels that might occur to a larger extent during later phases of tumor growth.

In the absence of increased vessel density in tumors derived from PDGF-transfected cells, the tumor growth-stimulatory effect of PDGF is best explained by functional rather than quantitative changes of the tumor vasculature. In a recent detailed characterization of tumor vessels in experimental tumors, different categories of tumor vessels were characterized (46). Nonperfused endothelial cell sprouts that lacked pericyte coverage were the least functional of these vessel categories. It is thus possible that the tumor growth-stimulatory effects of PDGF in the B16 model involve increased functionality of tumor vessels through a decrease in the fraction of nonperfused vessels. Alternatively, other aspects of the functionality of endothelial cells might be improved through maturation signals derived from pericytes.

According to experimental therapy studies, the antiangiogenic effects of agents targeting endothelial cells are much more effective on immature vessels, which are characterized by low pericyte coverage (46, 47). These findings, together with the observations of the present study, suggest that a combination of vascular endothelial growth factor receptor-targeting drugs with PDGF receptor inhibitors constitutes a rational combination for antiangiogenic tumor therapy. In support of this notion, therapeutic benefits were recently observed after combination of vascular endothelial growth factor receptor antagonists with STI571 in a genetic model of insulinoma, presumably through STI571-mediated targeting of PDGF receptors on pericytes (48, 49).

In conclusion, our findings provide evidence for a role of tumor-derived PDGF-BB and PDGF-DD in pericyte recruitment to tumor vessels. Our data also suggest that increased pericyte density may improve tumor vessel functionality and enhance tumor growth rate. The therapeutic implications of these findings merit further investigations.

## ACKNOWLEDGMENTS

We thank Kristian Pietras and Carina Hellberg for critical reading of the manuscript and Ingegård Schiller for expert secretarial assistance.

## REFERENCES

- Heldin C-H, Östman A, Rönstrand L. Signal transduction via platelet-derived growth factor receptors. *Biochim Biophys Acta* 1998;1378:F79-113.
- Pietras K, Sjöblom T, Rubin K, Heldin C-H, Östman A. PDGF receptors as cancer drug targets. *Cancer Cell* 2003;3:439-43.
- Buchdunger E, Zimmermann J, Mett H, et al. Inhibition of the Abl protein-tyrosine kinase in vitro and in vivo by a 2-phenylaminopyrimidine derivative. *Cancer Res* 1996;56:100-4.
- Östman A, Heldin C-H. Involvement of platelet-derived growth factor in disease: development of specific antagonists. *Adv Cancer Res* 2001;80:1-38.
- Capdeville R, Buchdunger E, Zimmermann J, Matter A. Glivec (STI571, imatinib), a rationally developed, targeted anticancer drug. *Nat Rev Drug Discov* 2002;1:493-502.
- Bergsten E, Uutela M, Li X, et al. PDGF-D is a specific, protease-activated ligand for the PDGF  $\beta$ -receptor. *Nat Cell Biol* 2001;3:512-6.
- LaRochelle WJ, Jeffers M, McDonald WF, et al. PDGF-D, a new protease-activated growth factor. *Nat Cell Biol* 2001;3:517-21.
- Li X, Pontén A, Aase K, et al. PDGF-C is a new protease-activated ligand for the PDGF  $\alpha$ -receptor. *Nat Cell Biol* 2000;2:302-9.
- Heldin C-H, Westermark B. Mechanism of action and in vivo role of platelet-derived growth factor. *Physiol Rev* 1999;79:1283-316.
- Gilbertson DG, Duff ME, West JW, et al. Platelet-derived growth factor C (PDGF-C), a novel growth factor that binds to PDGF  $\alpha$  and  $\beta$  receptor. *J Biol Chem* 2001;276:27406-14.
- Sjöblom T, Shimizu A, O'Brien KP, et al. Growth inhibition of dermatofibrosarcoma protuberans tumors by the platelet-derived growth factor receptor antagonist STI571 through induction of apoptosis. *Cancer Res* 2001;61:5778-83.
- Greco A, Fusetti L, Villa R, et al. Transforming activity of the chimeric sequence formed by the fusion of collagen gene COL1A1 and the platelet derived growth factor b-chain gene in dermatofibrosarcoma protuberans. *Oncogene* 1998;17:1313-9.
- Kilic T, Alberta JA, Zdunek PR, et al. Intracranial inhibition of platelet-derived growth factor-mediated glioblastoma cell growth by an orally active kinase inhibitor of the 2-phenylaminopyrimidine class. *Cancer Res* 2000;60:5143-50.
- Shamah SM, Stiles CD, Guha A. Dominant-negative mutants of platelet-derived growth factor revert the transformed phenotype of human astrocytoma cells. *Mol Cell Biol* 1993;13:7203-12.
- Shimizu A, O'Brien KP, Sjöblom T, et al. The dermatofibrosarcoma protuberans-associated collagen type I $\alpha$ 1/platelet-derived growth factor (PDGF) B-chain fusion gene generates a transforming protein that is processed to functional PDGF-BB. *Cancer Res* 1999;59:3719-23.
- Maki RG, Awan RA, Dixon RH, Jhanwar S, Antonescu CR. Differential sensitivity to imatinib of 2 patients with metastatic sarcoma arising from dermatofibrosarcoma protuberans. *Int J Cancer* 2002;100:623-6.
- Rubin BP, Schuetz SM, Eary JF, et al. Molecular targeting of platelet-derived growth factor B by imatinib mesylate in a patient with metastatic dermatofibrosarcoma protuberans. *J Clin Oncol* 2002;20:3586-91.
- Skobe M, Fusenig NE. Tumorigenic conversion of immortal human keratinocytes through stromal cell activation. *Proc Natl Acad Sci USA* 1998;95:1050-5.
- Forsberg K, Vally-Nagy I, Heldin C-H, Herlyn M, Westermark B. Platelet-derived growth factor (PDGF) in oncogenesis: development of a vascular connective tissue stroma in xenotransplanted human melanoma producing PDGF-BB. *Proc Natl Acad Sci USA* 1993;90:393-7.
- Pietras K, Östman A, Sjöquist M, et al. Inhibition of platelet-derived growth factor receptors reduces interstitial hypertension and increases transcapillary transport in tumors. *Cancer Res* 2001;61:2929-34.
- Pietras K, Rubin K, Sjöblom T, et al. Inhibition of PDGF receptor signaling in tumor stroma enhances antitumor effect of chemotherapy. *Cancer Res* 2002;62:5476-84.
- Pietras K, Stumm M, Hubert M, et al. STI571 enhances the therapeutic index of epothilone B (EPO906) by a tumor-selective increase of drug uptake. *Clin Cancer Res* 2003;9:3779-87.
- Battegay EJ, Rupp J, Iruela-Arispe L, Sage EH, Pech M. PDGF-BB modulates endothelial proliferation and angiogenesis in vitro via PDGF  $\beta$ -receptors. *J Cell Biol* 1994;125:917-28.
- Risau W, Drexler H, Mironov V, et al. Platelet-derived growth factor is angiogenic in vivo. *Growth Factors* 1992;7:261-6.
- Cao R, Brakenhielm E, Li X, et al. Angiogenesis stimulated by PDGF-CC, a novel member in the PDGF family, involves activation of PDGFR- $\alpha$  and - $\beta$  receptors. *FASEB J* 2002;16:1575-83.
- Lindahl P, Johansson BR, Levee P, Betsholtz C. Pericyte loss and microaneurysm formation in PDGF-B-deficient mice. *Science (Wash DC)* 1997;277:242-5.
- Hellström M, Kalén M, Lindahl P, Abramsson A, Betsholtz C. Role of PDGF-B and PDGFR- $\beta$  in recruitment of vascular smooth muscle cells and pericytes during embryonic blood vessel formation in the mouse. *Development* 1999;126:3047-55.
- Enge M, Bjarnegård M, Gerhardt H, et al. Endothelium-specific platelet-derived growth factor-B ablation mimics diabetic retinopathy. *EMBO J* 2002;21:4307-16.
- Sundberg C, Ljungström M, Lindmark G, Gerdin B, Rubin K. Microvascular pericytes express platelet-derived growth factor- $\beta$  receptors in human healing wounds and colorectal adenocarcinoma. *Am J Pathol* 1993;143:1377-88.

30. Abramsson A, Berlin O, Papayan H, et al. Analysis of mural cell recruitment to tumor vessels. *Circulation* 2002;105:112-7.
31. Hermanson M, Funa K, Hartman M, et al. Platelet-derived growth factor and its receptors in human glioma tissue: expression of messenger RNA and protein suggests the presence of autocrine and paracrine loops. *Cancer Res* 1992;52:3213-9.
32. Uehara H, Kim SJ, Karashima T, et al. Effects of blocking platelet-derived growth factor-receptor signaling in a mouse model of experimental prostate cancer bone metastases. *J Natl Cancer Inst (Bethesda)* 2003;95:458-70.
33. Guo P, Hu B, Gu W, et al. Platelet-derived growth factor-B enhances glioma angiogenesis by stimulating vascular endothelial growth factor expression in tumor endothelia and by promoting pericyte recruitment. *Am J Pathol* 2003;162:1083-93.
34. Li H, Fredriksson L, Li X, Eriksson U. PDGF-D is a potent transforming and angiogenic growth factor. *Oncogene* 2003;22:1501-10.
35. Thyberg J, Östman A, Bäckström G, Westermarck B, Heldin, C-H. Localization of platelet-derived growth factor (PDGF) in CHO cells transfected with PDGF A- or B-chain cDNA: retention of PDGF-BB in the endoplasmic reticulum and Golgi complex. *J Cell Sci* 1990;97:219-29.
36. Workman P, Balmain A, Hickman JA, et al. UKCCCR guidelines for the welfare of animals in experimental neoplasia. *Lab Anim* 1988;22:195-201.
37. Heuchel R, Berg A, Tallquist M, et al. Platelet-derived growth factor  $\beta$  receptor regulates interstitial fluid homeostasis through phosphatidylinositol-3' kinase signaling. *Proc Natl Acad Sci USA* 1999;96:11410-5.
38. Gundersen HJG, Bendtsen TF, Korbo L, et al. Some new, simple and efficient stereological methods and their use in pathological research and diagnosis. *APMIS* 1988;96:379-94.
39. Wassberg E, Hedborg F, Skoldenberg E, Stridsberg M, Christofferson R. Inhibition of angiogenesis induces chromaffin differentiation and apoptosis in neuroblastoma. *Am J Pathol* 1999;154:395-403.
40. Schlingemann RO, Rietveld FJ, de Waal RM, Ferrone S, Ruiter DJ. Expression of the high molecular weight melanoma-associated antigen by pericytes during angiogenesis in tumors and in healing wounds. *Am J Pathol* 1990;136:1393-405.
41. Schlingemann RO, Rietveld FJR, Kwaspen F, et al. Differential expression of markers for endothelial cells, pericytes, and basal lamina in the microvasculature of tumors and granulation tissue. *Am J Pathol* 138:1335-47.
42. Eberhard A, Kahlert S, Goede V, et al. Heterogeneity of angiogenesis and blood vessel maturation in human tumors: implications for antiangiogenic therapies. *Cancer Res* 60:1388-93.
43. Shao Z-M, Nguyen M, Barsky SH. Human breast carcinoma desmoplasia is PDGF initiated. *Oncogene* 2000;19:4337-45.
44. Nicosia RF, Nicosia SV, Smith M. Vascular endothelial growth factor, platelet-derived growth factor, and insulin-like growth factor-I promote rat aortic angiogenesis *in vitro*. *Am J Pathol* 1994;145:1023-9.
45. Abramsson A, Lindblom P, Betsholtz C. Endothelial and non-endothelial sources of PDGF-B regulate pericyte recruitment and influence vascular pattern formation in tumors. *J Clin Invest* 2003;112:1142-51.
46. Gee MS, Procopio WN, Makonnen S, et al. Tumor vessel development and maturation impose limits on the effectiveness of anti-vascular therapy. *Am J Pathol* 2003; 162:183-93.
47. Benjamin LE, Golijanin D, Itin A, Podes D, Keshet E. Selective ablation of immature blood vessels in established human tumors follows vascular endothelial growth factor withdrawal. *J Clin Invest* 1999;103:159-65.
48. Bergers G, Song S, Meyer-Morse N, Bergsland E, Hanahan D. Benefits of targeting both pericytes and endothelial cells in the tumor vasculature with kinase inhibitors. *J Clin Invest* 2003;111:1287-95.
49. Erber R, Thurner A, Katsen AD, et al. Combined inhibition of VEGF- and PDGF-signaling enforces tumor vessel regression by interfering with pericyte-mediated endothelial cell survival mechanisms. *FASEB J* 2004;18:338-40.